PRAMANA
— journal of
physics



Vol. 64, No. 6
June 2005
pp. 971–980

# The depletion potential in one, two and three dimensions

R ROTH[1,2] and P-M KÖNIG[1,2]
[1]Max-Planck-Institut für Metallforschung, Heisenbergstr. 3, 70569 Stuttgart, Germany
[2]Institut für Theoretische und Angewandte Physik, Universität Stuttgart,
Pfaffenwaldring 57, 70569 Stuttgart, Germany
E-mail: Roland.Roth@mf.mpg.de

**Abstract.** We study the behavior of the depletion potential in binary mixtures of hard particles in one, two, and three dimensions within the framework of a general theory for depletion potential using density functional theory. By doing so we extend earlier studies of the depletion potential in three dimensions to the cases of $d = 1$ and 2 about which little is known, despite their importance for experiments. We also verify scaling relations between depletion potentials in sphere–sphere and wall–sphere geometries in $d = 3$ and in disk–disk and wall–disk geometries in $d = 2$, which originate from geometrical considerations.

**Keywords.** Colloids; depletion potential; density functional theory.

**PACS Nos 82.70.Dd; 61.20.Gy**

## 1. Introduction

Colloids are often considered as ideal model systems for studying structural and thermodynamic properties of liquids because the interaction between colloidal particles can be tuned to a great extent. By changing the properties of the solvent, it is possible to influence dispersion forces and screen off electrostatic interactions so that the resulting effective bare interaction between colloids can be hard-sphere like. Adding smaller colloids to the suspension can further influence the effective interaction between the bigger colloids by introducing the so-called depletion forces, as was first pointed out by Asakura and Oosawa [1] theoretically 50 years ago. In the meantime depletion forces are well-studied in three-dimensional colloidal suspensions both theoretically [2] and experimentally [3,4]. In recent experiments with a colloid–polymer mixture [3] and in a mixture of big spherical and small rod-like colloids [4] it was established that the theory of depletion forces [2,5] and results from measurements are in quantitative agreement.

Recent progress in experimental techniques made it possible to confine colloids to two [6] and even one dimensions [7] using light forces and to observe

the particles with video microscopy. This development opens the opportunity to also study depletion forces in one and two dimensions. Theoretical work, however, focused so far mainly on the three-dimensional case, with the exception of ref. [8] where depletion forces in $d = 2$ were studied using integral equations and simulations.

Here we want to fill the gap and present a study of the depletion potential in one, two and three dimensions within the same approach. This allows us to understand which features are common to all cases and which are special. In $d = 1$ we obtain the exact depletion potential which can help to understand better some characteristics in two and three dimensions, where results can be obtained only numerically from approximate theories. In §2 we present our general theoretical approach to depletion potentials [2] and specify the density functionals we apply in one and two dimensions, since they are lesser known than their three-dimensional counterpart. Our results are presented in §3. We conclude with a discussion in §4.

## 2. Theory

We follow the general approach [2] to depletion potentials between two big particles in a sea of small ones using the potential distribution theorem [9,10] within the framework of density functional theory. To this end we require a density profile of small particles around a single big one and a density functional for the intrinsic excess free energy $\mathcal{F}_{\rm ex}^{(d)}[\{\rho_i\}]$ for a mixture [2] in $d$ dimensions. The depletion potential is then given by [2]

$$\beta W^{(d)}(\mathbf{r}) = \lim_{\rho_b \to 0} (c_b^{(1)}(\mathbf{r} \to \infty) - c_b^{(1)}(\mathbf{r})), \tag{1}$$

and $c_b^{(1)}(\mathbf{r}) = -\beta\delta\mathcal{F}_{\rm ex}^{(d)}/\delta\rho_b(\mathbf{r})$ is the one-body direct correlation function, and $\beta = 1/(k_{\rm B}T)$. In the present study we are interested in mixtures of hard particles with radius $R$ in three, two and one dimensions, which are named spheres, disks and rods, respectively. In all three cases, $d = 1, \ldots, 3$, the structure of $\mathcal{F}_{\rm ex}^{(d)}$ is given by

$$\beta\mathcal{F}_{\rm ex}^{(d)}[\{\rho_i\}] = \int \mathrm{d}\mathbf{r}\ \Phi^{(d)}(\{n_\alpha^{(d)}\}), \tag{2}$$

where the excess free energy density $\Phi^{(d)}$ is a function of weighted densities

$$n_\alpha^{(d)}(\mathbf{r}) = \sum_i \int \mathrm{d}\mathbf{r}' \rho(\mathbf{r}') w_{\alpha,i}^{(d)}(\mathbf{r}, \mathbf{r}'), \tag{3}$$

and $i = 1, \ldots, N$ counts the components.

The *exact* one-dimensional functional due to Percus [11] and Vanderlick [12] is given by

$$\Phi^{(1d)} = -n_0^{(1d)} \ln(1 - n_3^{(1d)}), \tag{4}$$

with the corresponding weight functions $w_{0,i}^{(1d)}(x) = [\delta(x - R_i) + \delta(x + R_i)]/2$ and $w_{3,i}^{(1d)}(x) = \Theta(|R_i - x|)$. This form of the excess free energy inspired Rosenfeld [13] to formulate a density functional for a hard-sphere mixture in $d = 3$, which he later adapted to the case of hard-disk mixtures in $d = 2$ [14]. Because these functionals use weight functions that depend on the fundamental geometrical measures of individual particles they are also known as fundamental measure theory (FMT).

In two dimensions we use the FMT functional of ref. [14]

$$\Phi^{(2d)} = -n_0^{(2d)} \ln(1 - n_3^{(2d)}) + \frac{n_2^{(2d)} n_2^{(2d)} - \mathbf{n}_2^{(2d)} \cdot \mathbf{n}_2^{(2d)}}{4\pi(1 - n_3^{(2d)})}, \tag{5}$$

with three scalar weight functions $w_{3,i}^{(2d)}(r) = \Theta(R_i - r)$, $w_{2,i}^{(2d)}(r) = \delta(R_i - r)$, $w_{0,i}^{(2d)}(r) = w_{2,i}^{(2d)}(r)/(2\pi R_i)$ and one vectorial weight function $\mathbf{w}_{2,i}^{(2d)}(r) = \mathbf{r}/r\delta(R_i - r)$.

In three dimensions we use the so-called White-Bear version of FMT [15,16] which improves the original version of FMT by Rosenfeld [13] as it enforces the accurate MCSL equation of state [17] and hence improves the predictions of the functional especially at high packing fractions over those from the original version of FMT. For details on that functional we refer the reader to refs [15,16].

Combining eqs (1)–(3), we can write the depletion potential for FMT functionals as

$$\beta W^{(d)}(\mathbf{r}) = \sum_\alpha \int \mathbf{r}' \left[ \left( \frac{\beta \partial \Phi^{(d)}}{\partial n_\alpha^{(d)}} \right)_{\mathbf{r}'} - \left( \frac{\beta \partial \Phi^{(d)}}{\partial n_\alpha^{(d)}} \right)_\infty \right] w_{\alpha,b}^{(d)}(\mathbf{r}', \mathbf{r}), \tag{6}$$

which was used to great effect in $d = 3$ for additive [2] as well as for non-additive [18] spheres. Here we want to extend this study to the one- and two-dimensional cases and study which features of the depletion potential, in all dimensions, are common and those that are special to one particular case.

## 3. Results

The first step in obtaining the depletion potential is the calculation of the density profile of small particles at a given number density $\rho$ around a single fixed big one with radius $R_b$. This step is important and allows us to test the accuracy of the functional as well as that of the numerics. In $d = 1$ the functional is exact and the required numerics is rather simple. So we do not report details about the density profile here but merely mention one peculiarity in $d = 1$, namely that the external potential acting on the small particles originating from fixing a small or a big particle or from a hard wall is the same except for a trivial shift along the $x$-axis. Hence, $\rho^{(1d)}(x)$ is independent of the size of the big particle.

Density profiles in three dimensions obtained from FMT are well-studied [2,15,19] and so we focus here on the two-dimensional case for which little is known about the accuracy of the FMT density functional of ref. [14] with the exception of a

comparison between density profiles from DFT with those from simulations inside a circular cavity in ref. [20].

We perform calculations of the density profile of a fluid of small disks, $\rho^{(2d)}(r)$, around a single big disk with radius $R_b$ fixed at the origin as a function of the packing fraction $\eta^{(2d)} = \rho R^2\pi$ and $R_b$. We established that our DFT program satisfies accurately the contact sum-rule [10,21] that relates the density of small disks in contact with the big disk $\rho_c^{(2d)}$, which is a microscopic quantity, with thermodynamic quantities of the fluid. In our particular case the contact sum-rule reads

$$\rho_c^{(2d)} = \beta p + \frac{\beta\gamma(R_b+R)}{R_b+R} + \left.\frac{\partial\gamma(R)}{\partial R}\right|_{R=R_b+R}, \tag{7}$$

where $\beta p$ is the equation of state that underlies the functional and we use the two-dimensional 'surface tension' $\gamma \equiv (\Omega + pV)/A$ with definitions of the 'volume' $V$ (the surface area available to the centers of the small disks) and the surface 'area' $A$ (the circumference of a disk with radius $R_b + R$) corresponding to a dividing surface at the position where the density profile jumps. This test ensures that the numerical implementation of DFT is self-consistent and accurate. In order to test the accuracy of the functional we perform canonical Monte-Carlo simulations to determine the density profiles of a one-component hard-disk fluid around a single big disk. Our results for different values of $\eta^{(2d)}$ and $R_b = 3R$ are shown in figure 1. We find that the

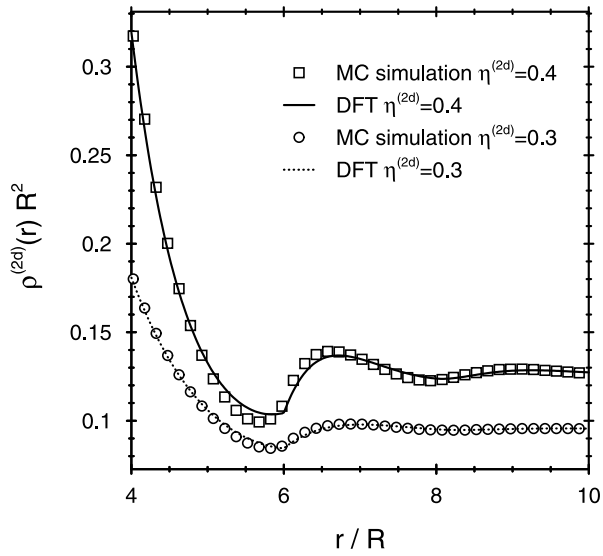


**Figure 1.** Density profiles of a fluid of hard disks around a single fixed big disk with radius $R_b = 3R$ as obtained from DFT (lines) and from canonical Monte-Carlo simulations (symbols) at two packing fractions $\eta^{(2d)} = \rho R^2\pi$. Close to contact the agreement is very good, however, $2R$ away from contact the present DFT over-emphasizes the cusp in the density profile. The overall agreement between both results is good.

overall agreement between DFT results and those from simulations is good. Close to contact the agreement is especially good. The density profiles obtained from DFT systematically over-emphasize the cusp at $r = R_b + 2R$ away from contact. This might have to do with the fact that in two dimensions the Mayer-f bond cannot be deconvolved exactly with a finite number of weight functions [14], a point that should be further investigated in the future. It is interesting to note that density profiles in $d = 2$ depend only weakly on curvature and reach the planar limit rather quickly.

Now we turn to our results on depletion potentials. We start with the one-dimensional case for which the exact DFT, eq. (4), allows us to calculate the exact depletion potential [22], which we show in figure 2 for various values of the packing fraction $\eta^{(1d)} = \rho 2R$. Note that in one dimension the depletion potential is independent of the size ratio $q = R/R_b$ so that $\eta^{(1d)}$ is the only parameter. From the exact expression for the depletion potential we can specify two important properties of the depletion potential in closed form, namely the contact value

$$\beta W_0^{(1d)} = \beta W^{(1d)}(h = 0) = \ln(1 - \eta^{(1d)}), \tag{8}$$

which is always negative for $\eta^{(1d)} > 0$, and the height of the repulsive potential barrier $\Delta W_\mathrm{r}$ [23], which in $d = 1$ is located precisely at $h = 2R$,

$$\beta \Delta W_\mathrm{r}^{(1d)} = \beta W^{(1d)}(h = 2R) = \ln(1 - \eta^{(1d)}) + \frac{\eta^{(1d)}}{1 - \eta^{(1d)}}. \tag{9}$$

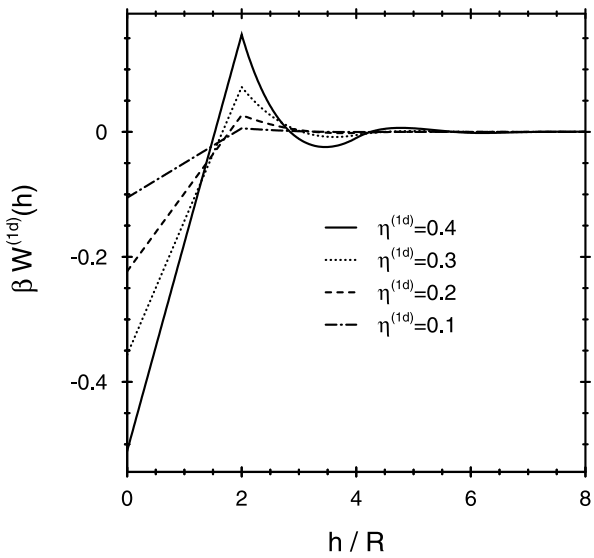


**Figure 2.** The exact depletion potential in $d = 1$ for various values of $\eta^{(1d)} = \rho 2R$. In one dimension, the depletion potential depends only on $\eta^{(1d)}$ and is independent of the size ratio $q = R/R_b$. The contact value and the value of the depletion potential at $h = 2R$ are given by eqs (8) and (9), respectively.

For small separation between the big particles, $h \leq 2R$, the depletion potential increases linearly with $h$ and the slope is given by the pressure. At $h = 2R$ there is a cusp, caused by the fact that for $h \geq 2R$ there can be small particles between two big ones, while for $h < 2R$ there are none and reducing the separation $h$ between the big particles increases the accessible 'volume' for the small spheres in the system linearly and causes the grand potential of the system to increase correspondingly. This argument cannot be applied in higher dimensions. For larger separations, $h > 2R$, the depletion potential displays an exponentially damped oscillatory behavior [2] which is set by the asymptotic behavior of the density profile of the small particles at a single wall or particle.

In two dimensions our results for the depletion potential are obtained numerically from DFT. We show the depletion potential between two big disks in a sea of small disks with a size ratio $q = R/R_b = 0.2$ in figure 3. Again we find a cusp at $h = 2R$, which however, seems to be over-emphasized by the approximate DFT similar to the case of the density profiles shown in figure 1. In the region $h < 2R$ the behavior of the depletion potential is not linear as in $d = 1$ and the deviation from linearity becomes more pronounced with increasing packing fraction. In $d > 1$ the depletion potential depends, in addition to the packing fraction, also on the size ratio $q = R/R_b$ between the small and the big particles. The depth of the depletion potential at contact as well as the height of the potential barrier and the amplitude of the oscillations for $h > 2R$ increase as $q$ decreases. In ref. [8] the disk–disk depletion potential within Asakura–Oosawa (AO) [1] approximation was given. This approximation neglects correlation effects and hence is valid for small packing fractions of the small particles. An excellent approximation for the contact

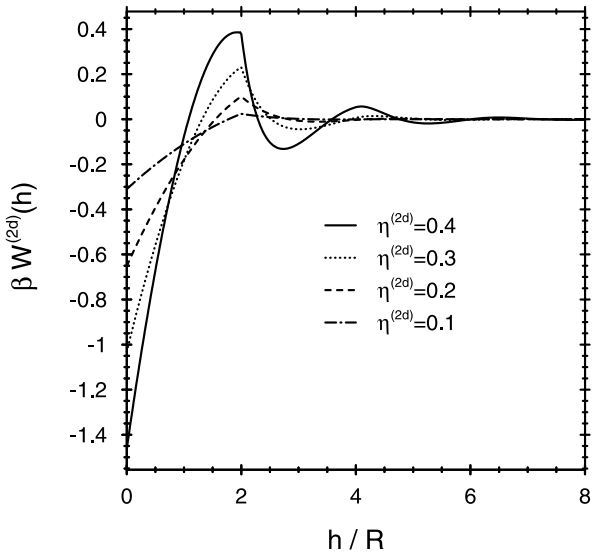


**Figure 3.** The depletion potential in two dimensions as calculated from DFT for various values of $\eta^{(2d)} = \rho R^2 \pi$ and a size ratio $q = R/R_b = 0.2$. The cusp at $h = 2R$ results in a jump of the depletion force at this position.

value $\beta W_{\rm AO}^{(2d)}(h=0) \approx -\eta^{(2d)}\ 2/\pi(1.88562/\sqrt{q}+0.65996\sqrt{q})$ was given for $q < 0.5$ and $\eta^{(2d)} \to 0$ [8]. Here we propose an empirical parametrization for the contact value of the disk–disk depletion potential in $d = 2$ by using the geometrical factor of the Asakura–Oosawa potential and the dependency on the packing fraction of the small disks from the exact one-dimensional result, eq. (8), and we obtain

$$\beta W_0^{(2d)} = \beta W^{(2d)}(h=0) \approx \ln(1-\eta^{(2d)})\ \frac{2}{\pi}\left(\frac{1.88562}{\sqrt{q}} + 0.65996\sqrt{q}\right), \tag{10}$$

which recovers the Asakura–Oosawa results for small values of $\eta^{(2d)}$ and is in excellent agreement with our numerical results obtained from DFT up to a packing fraction of $\eta^{(2d)} = 0.5$ and for all size ratios we studied down to $q = 0.1$.

A comparison between our results for the $d = 2$ depletion potential and that from ref. [8] shows that the results are similar, but the agreement clearly is not quantitative. One difference between the present results and those from ref. [8] is that the depletion force from DFT is discontinuous at $h = 2R$ whereas it is continuous from integral equations and from simulations in ref. [8].

In figure 4 we compare the disk–disk depletion potential (dotted line) with the corresponding wall–disk result (full line) for a size ratio $q = 0.2$ and a disk packing fraction of $\eta = 0.3$. Purely geometrical arguments within the Asakura–Oosawa approximation predict that the wall–disk potential has to be more attractive for

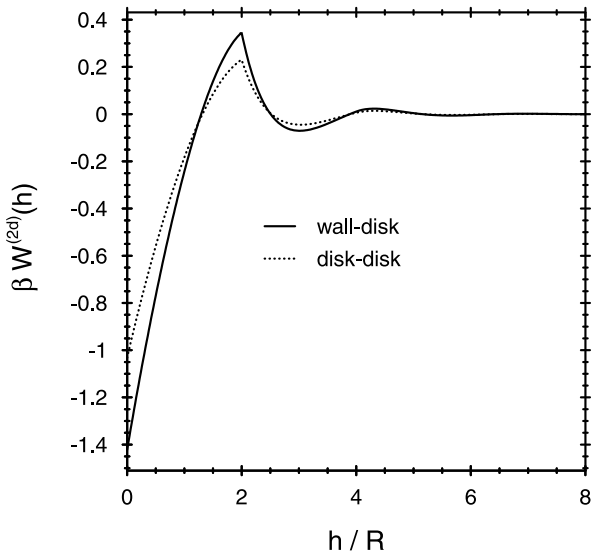


**Figure 4.** A comparison between the disk–disk (dotted line) and the wall–disk (full line) depletion potential for $\eta^{(2d)} = 0.3$ and $q = R/R_b = 0.2$. If $q$ is small enough, one can obtain the wall–disk depletion potential from the corresponding disk–disk results by multiplying it by a geometrical scaling factor of $\sqrt{2}$.

small values of $h$ than the disk–disk potential. For small enough size ratios $q$ there is a simple scaling between these two results and we find the scaling factor to be $\sqrt{2}$ to leading order in $q$, i.e. the wall–disk potential can be obtained by multiplying the disk–disk result by $\sqrt{2}$. We verified this scaling behavior for the potentials shown in figure 4 as well as for many other potentials at different values of $\eta^{(2d)}$ and different size ratios $q$. It is also interesting to note that, given $q$ is small enough, the same scaling holds to a very good approximation between a disk–disk depletion potential with size ratio $q$ and one with size ratio $q' = q/2$, i.e., the wall–disk depletion potential shown in figure 4 is almost indistinguishable from a disk–disk potential at the same packing fraction but a size ratio $q = 0.1$.

We show the well-studied [2] case of a sphere–sphere depletion potential in $d = 3$ for various values of $\eta^{(3d)} = \rho 4\pi/3R^3$ in figure 5. The potential is smooth even at $h = 2R$, but the force, i.e., the negative of its derivative w.r.t. $h$, displays a cusp at this position [2]. $W^{(3d)}(h)$ shows an even stronger dependency on the size ratio $q$ than its two-dimensional counterpart. For a given size ratio and packing fraction the potential at contact is more negative in $d = 3$ than in $d = 2$, which is more negative than the potential in one dimension, i.e. $W^{(3d)}(h = 0) < W^{(2d)}(h = 0) < W^{(1d)}(h = 0)$. The first potential barrier is also most pronounced in $d = 3$ as can be seen in figures 2, 3 and 5. The position of the first potential barrier is located at a position $h < 2R$ which strongly depends on $\eta^{(3d)}$: for small values of $\eta^{(3d)}$ it is located at $h \approx 2R$, while it is at $h \approx R$ for $\eta^{(3d)} = 0.4$, as is shown in figure 5.

For the three-dimensional depletion potential it is known that for a sufficiently small size ratio $q$ there is a scaling between the wall–sphere and sphere–sphere geometry with a scaling factor of 2 to leading order in $q$, i.e. the difference between these two geometries is stronger than in $d = 2$, where the scaling factor is $\sqrt{2}$.

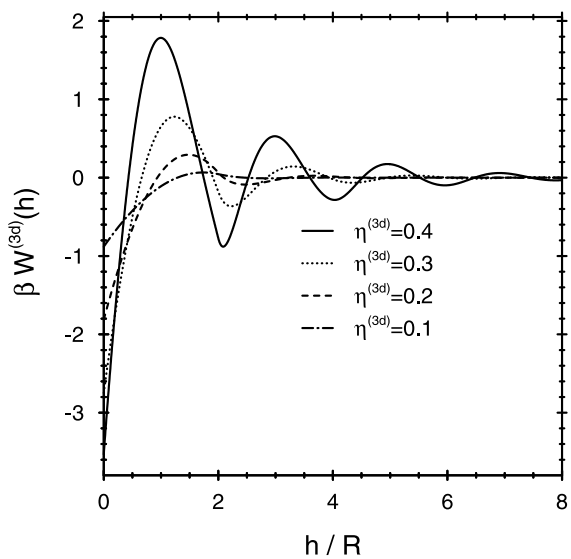


**Figure 5.** The depletion potential between two spheres in three dimensions for various values of $\eta^{(3d)} = \rho 4\pi/3R^3$ and a size ratio $q = R/R_b = 0.2$.

The same scaling holds, as in the two-dimensional case, to a good approximation between two sphere–sphere depletion potentials with size ratios $q$ and $q' = q/2$.

## 4. Discussion

We have presented depletion potentials between hard spheres in $d = 3$, between hard disks in $d = 2$ and between hard rods in $d = 1$ obtained from the same general approach within FMT. We find that in all three cases the depletion potentials have some common features: at short distances the potential is always attractive and the contact value at $h = 0$ depends on the packing fraction and in $d = 2$ and 3 also on the size ratio $q$. The depletion potential increases monotonically until the first potential barrier at $h = 2R$ in $d = 1$ and at $h \leq 2R$ in $d = 2$ and 3. From the first potential barrier to $h \to \infty$ the depletion potential displays an exponentially damped oscillatory behavior which is given by the asymptotic decay of the density profile of the small particles around a single big one [2].

In $d = 1$ we give the exact contact value of the depletion potential and the exact value at the first potential barrier at $h = 2R$. From the result in one dimension, we give an empirical parametrization of the potential at contact in $d = 2$, which is in excellent agreement with our numerical findings. In three dimension the behavior is more complicated at high values of the packing fraction which prohibits a simple parametrization along similar lines.

We verify that in $d = 3$ the sphere–sphere and the wall–sphere potentials and in $d = 2$ the disk–disk and wall–disk potentials are related through a simple geometrical scaling with a factor of 2 and $\sqrt{2}$, respectively. A similar scaling also connects sphere–sphere or disk–disk depletion potentials with size ratios $q$ and $q' = q/2$.

## Acknowledgements

It is a pleasure to acknowledge useful discussions with Ramon Castañeda-Priego.

## References

[1] S Asakura and F Oosawa, *J. Chem. Phys.* **22**, 1255 (1954)
[2] R Roth, R Evans and S Dietrich, *Phys. Rev.* **E62**, 5360 (2000)
[3] C Bechinger, D Rudhardt, P Leiderer, R Roth and S Dietrich, *Phys. Rev. Lett.* **83**, 3960 (1999)
[4] L Helden, R Roth, G H Koenderink, P Leiderer and C Bechinger, *Phys. Rev. Lett.* **90**, 048301 (2003)
[5] R Roth, *J. Phys.: Condens. Matter* **15**, S277 (2003)
[6] M Brunner, C Bechinger, W Strepp, V Lobaskin and H H von Grünberg, *Europhys. Lett.* **58**, 926 (2002)
[7] C Lutz, M Kollmann and C Bechinger, *Phys. Rev. Lett.* **93**, 026001 (2004).
[8] R Castañeda-Priego, A Rodriguez-Lopez and J M Mendez-Alcaraz, *J. Phys.: Condens. Matter* **15**, S3393 (2003)

[9] B Widom, *J. Phys. Chem.* **86**, 869 (1982)
[10] J R Henderson, *Mol. Phys.* **50**, 741 (1983)
[11] J K Percus, *J. Stat. Phys.* **15**, 505 (1976)
[12] T K Vanderlick, H T Davis and J K Percus, *J. Chem. Phys.* **91**, 7136 (1989)
[13] Y Rosenfeld, *Phys. Rev. Lett.* **63**, 980 (1989)
[14] Y Rosenfeld, *Phys. Rev.* **A42**, 5978 (1990)
[15] R Roth, R Evans, A Lang and G Kahl, *J.Phys.: Condens. Matter* **14**, 12063 (2002)
[16] Y-X Yu and J Wu, *J. Chem. Phys.* **117**, 10156 (2002)
[17] G A Mansoori, N F Carnahan, K E Starling and T W Leland Jr., *J. Chem. Phys.* **54**, 1523 (1971)
[18] R Roth and R Evans, *Europhys. Lett.* **53**, 271 (2001)
[19] R Roth and S Dietrich, *Phys. Rev.* **E62**, 6926 (2000)
[20] S-C Kim, Z T Nemeth, M Heni and H Löwen, *Mol. Phys.* **99**, 1875 (2001)
[21] P Bryk, R Roth, K R Mecke and S Dietrich, *Phys. Rev.* **E68**, 031602 (2003)
[22] It is also possible to obtain a closed expression for the exact depletion potential in $d = 1$ without using DFT at all. Results along this line will be reported elsewhere
[23] R Roth, B Götzelmann and S Dietrich, *Phys. Rev. Lett.* **83**, 448 (1999)